On-chip integrated resonators for long-wave infrared photonics

Qiankun Liu, Joan Manel Ramírez, Vladyslav Vakarin, Xavier Le Roux, Jacopo Frigerio, Andrea Ballabio, Miguel Montesinos, Carlos Alonso-Ramos, Enrico Talamas Simola, Laurent Vivien, et al.

On-chip integrated resonators for long-wave infrared photonics

(Student Paper)

Qiankun Liu[1,*], Joan Manel Ramirez[1], Vladyslav Vakarin[1], Xavier Le Roux[1], Jacopo Frigerio[2], Andrea Ballabio[2], Miguel Montesinos[1], Carlos Alonso-Ramos[1], Enrico Talamas Simola[2], Laurent Vivien[1], Giovanni Isella[1], and Delphine Marris-Morini[1]

[1] Centre de Nanosciences et de Nanotechnologies (C2N), Université Paris Sud, CNRS, Université Paris Saclay, 91120 Palaiseau, France

[2] L-NESS, Dipartimento di Fisica, Politecnico di Milano, Polo di Como, Via Anzani 42, 22100 Como, Italy

e-mail: qiankun.liu@u-psud.fr

ABSTRACT

On-chip optical resonators are extensively applied to many fields such as light sources through lasing or enhancement of material nonlinear effects, chemical and biological sensing, and optical network monitoring. Silicon-based on-chip resonators have been reported previously in near infrared (NIR) and short-wave infrared (SWIR), however integrated resonant structures remain still challenging for long-wave infrared (LWIR). In this work, we experimentally demonstrate the first on-chip integrated resonators in LWIR up to 8.4 µm. Two types of resonators, Fabry-Perot cavities and racetrack ring resonators, have been both investigated. Maximum quality factors Q = 2200 and Q = 3200 have been respectively observed for Fabry-Perot cavity and racetrack ring resonator at a wavelength around 8 µm. These resonant structures lay the foundation for new generation of integrated photonics circuits that open the path towards miniaturized multi-functional LWIR systems.

Keywords: Integrated optics devices, Mid-infrared, Fabry-Perot cavities, Racetrack ring resonators.

1. INTRODUCTION

Mid-infrared silicon photonics is attracting a continuously increasing number of research activities due to its wide plethora of applications, including environmental monitoring, chemical and biological sensing, disease diagnosis and free space communication[1–3]. Among them, the identification of molecules through their unique absorption lines in the fingerprint region is particularly interesting for label-free on-chip sensing. However, the most used platform in silicon photonics, silicon-on-insulator, shows absorption at the wavelengths beyond 3.6 µm. In this context, alternative materials have been studied, such as suspended SOI, silicon nitride, III-V semiconductors, chalcogenides, Ge-on-Si, SiGe alloys and Ge-rich graded index SiGe. Among all pre-mentioned materials, Ge-rich graded index SiGe stands as a strong candidate for the demonstration of long-wave infrared operational photonic integrated circuits, due to i) its extended transparency potentially up to 15 µm; ii) high crystalline quality; iii) high 3rd order nonlinearity; iv) high versatility of optical engineering. Moreover, recent advances on graded index SiGe platform [4–6] report the experimental confirmation of its LWIR operation and show the potential for the investigation of LWIR integrated multi-target molecule detection systems.

To accomplish this task, on-chip mid infrared integrated resonator remains still challenging. Silicon-based on-chip resonators have been reported previously in near infrared (NIR) and short-wave infrared (SWIR), however the demonstration of LWIR resonators are still in its infancy. In this paper, we report our recent advance on the LWIR integrated resonators using graded index SiGe waveguides. Fabry-Perot cavities using waveguide Bragg gratings, and racetrack ring resonators have been experimentally demonstrated [7, 8]. Because of the low index contrast between graded waveguide core and silicon substrate, Bragg gratings must be carefully designed in the hand of Fabry-Perot cavities. Bragg grating waveguides up to 8.4 µm has been experimentally demonstrated, Fabry-Perot cavities with a loaded quality factor (Q) of 2200 are obtained at a wavelength around 7.95 µm. In the hand of ring resonators, resonators with R > 50 µm offer a high LWIR bandwidth of 900 nm, and display deep resonances with an extinction ratio (ER) up to 10 dB, a loaded quality factor of 3200 is measured at a wavelength around 8.05 µm. These results provide the feasibility of using graded-index SiGe waveguides for the demonstration of long-wave infrared resonant structures, opening the path towards the further implementation of advanced LWIR photonics integrated circuits.

2. Bragg grating waveguides and Fabry-Perot cavity

The Bragg grating waveguides are implemented on graded-index SiGe platform with Ge concentration linearly increasing from the Si substrate to pure Ge, across the 6-µm-thick waveguide core. Waveguides are then designed with 4 µm etch depth and 5 µm width. Bragg gratings corrugations are defined on top of the waveguide surface with a 400 nm etch depth and a duty cycle (DC) of 0.5. As the low vertical index contrast, an etch depth of 400 nm is chosen since it provides in the one hand a reasonable interaction between optical mode and the top-

surface waveguide corrugation, and in the other hand a good optical confinement of propagating mode in the corrugated waveguide. The interaction between optical mode and gratings can be descripted as coupling efficiency by the following equation:

$$K = \frac{\Gamma \times (n_h^2 + n_l^2) \times \sin(\pi \times DC)}{\lambda_B \times n_{eff}} \quad (1)$$

where Γ is the overlap factor between the guided optical mode and the grating region, n_h and n_l are the alternative high and low refractive index of two materials inside the grating region, DC is the duty cycle of corrugation, λ_B presents the Bragg wavelength and n_{eff} is the effective Bloch-Floquet mode at λ_B. The corrugation width is slightly narrower than the waveguide width ($W_{Corrug} < W_{WG}$), in order to improve the alignment tolerance between two layer lithography used in the fabrication process. Optimum corrugation width of Bragg gratings has been found by performing the numerical simulation. An optimized ratio ($r = W_{Corrug} / W_{WG}$) of 70% was obtained to maximize the coupling efficiency given by equation 1, corresponding to W_{Corrug} = 3.5 µm as shown in Figure 1(a).

The Bragg gratings and FP cavities were fabricated using an electron beam lithography, followed by an inductive coupled plasma (ICP) etching. The grating corrugations were firstly defined by a partial shallow-etch of 400 nm, a second etch step of 4 µm was then followed to define the waveguides. Figure 1(b) presents the scanning electron microscopy (SEM) picture of the fabricated Bragg gratings.

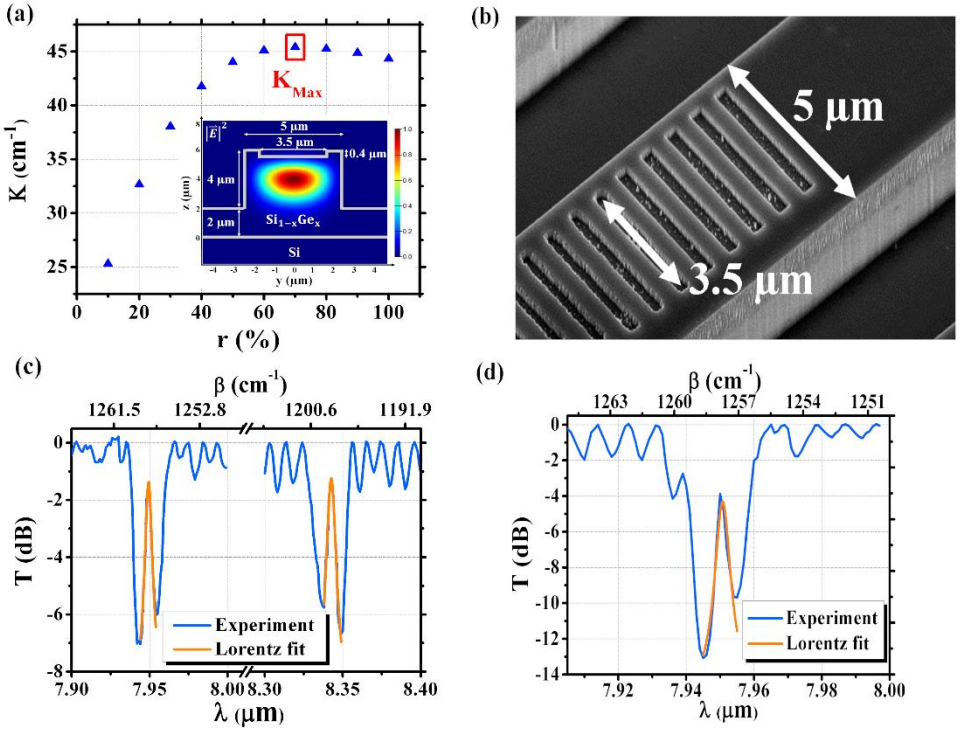

Figure 1. (a) Calculated coupling efficiency of the Bragg grating waveguide as a function of the ratio (r) between the shallow-etch corrugation width (W_{Corrug}) and the nominal waveguide width (W_{WG}) at a wavelength of 7.3 µm. Inset: Schematic of the waveguide cross-section with the simulated transverse magnetic (TM) mode profile in the grating region at 7.3 µm wavelength. (b) The SEM picture of a fabricated Bragg grating waveguide. (c) Measured transmittance spectrum of two different FP cavities with different design parameters: Λ = 1.1 µm (left), Λ = 1.16 µm (right), N = 280, L_{Cav} = 70 µm. Orange linese correspond to the Lorentzian fit of the central resonance. (d) Measured transmittance spectrum of a FP cavity with Λ = 1.1 µm, N = 500, L_{Cav} = 70 µm. The used Lorentzian function is:

$$y = y_0 + \frac{1}{\pi}\frac{2\Gamma}{\left[4\left(x - x_0\right)^2 + \Gamma^2\right]}$$

. The R-squared value of Lorentzian fit is 0.97.

Fabricated devices were characterized through a free-space configuration using a tenable external cavity quantum cascade laser (QCL). Figure 1(c) shows the experimental results of tow FP cavities with a number of periods (N) of 280, cavity length (L_{Cav}) of 70 µm and different grating period (Λ) 1.1 µm and 1.16 µm. Resonance peaks are measured at a wavelength of 7.95 µm and 8.35 µm, respectively. The -3 dB resonance bandwidths were measured to be 5.3 nm and 6.5 nm, corresponding to loaded quality factors of 1514 and 1272, respectively. The reflectivity of Bragg grating mirrors of around 88% and 85% can thus be estimated. The mirror losses can be also estimated by taking into account the maximum transmission about -1.3 dB at the resonant peak, and a propagation loss of 3 dB/cm ± 0.5 dB/cm [4]. The estimated mirror losses are between 1.2 and 1.8%.

Figure 1(d) presents the measurement result of a FP cavity with a number of periods of 500, keeping the same grating period and cavity length as presented previously in figure 1(c). The cavity Q-factor is improved by increasing the grating length, the -3 dB bandwidth at a resonance wavelength of 7.95 µm is reduced down to 3.6 nm, which yields a loaded Q-factor of 2200.

3. Racetrack resonator

Another approach, racetrack resonators have been also fabricated on the graded-index SiGe platform. Unlike the FP cavity using two Bragg mirrors implemented on a same waveguide, racetrack resonator is based on sing a directional coupler to couple light from the bus waveguide into the resonator. The resonators were fabricated through one step of lithography and ICP etch, with a etch depth of 3 µm and 4 µm waveguide width. Comparing to the previous FP cavity waveguide design, 1 µm shallower etch depth increases the coupling coefficient of the directional coupler which leads to a shorter coupler. Moreover, 4 µm waveguide width ensures the waveguide singlemode condition at interesting wavelength $\lambda \approx 8$ µm. The gap distance (L_{Gap}) and the length of directional coupler ($L_{Coupler}$) have been chosen as $L_{Gap} = 1$ µm and $L_{Coupler} = 200$ µm while considering the fabrication tolerance and the aspect ratio for the gap definition. Figure 2(a) and (b) show the SEM image of the fabricated resonators on top-view and the cross-section of a test resonator at directional coupler area, respectively.

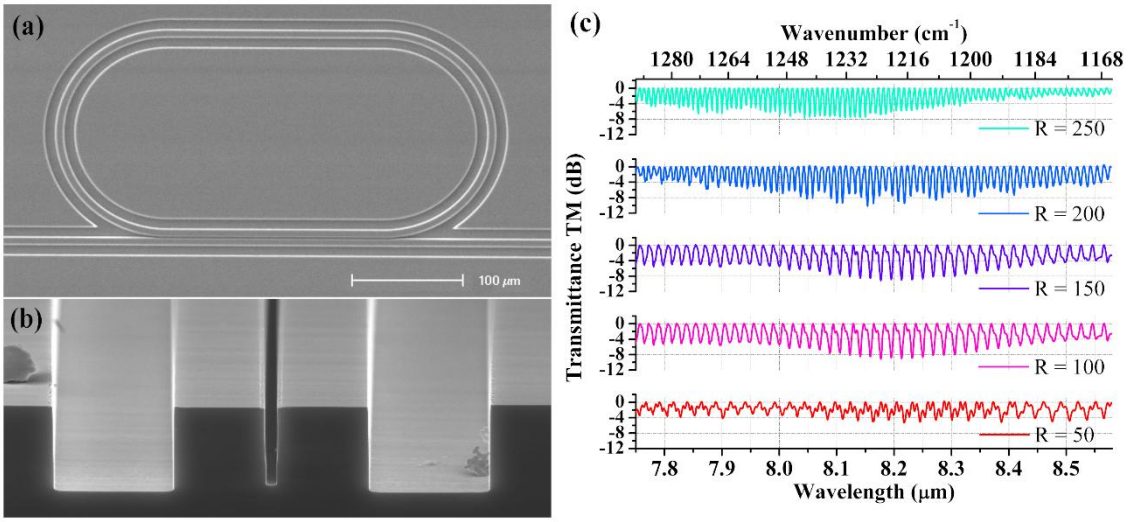

Figure 2. SEM image of the racetrack resonator (a) top view (b) cross-section of a test resonator device at the coupling area. (c) Experimental transmittance spectra of racetrack resonators with different bending radius, from bottom-up R = 50 µm (red), R = 100 µm (purple), R = 150 µm (violet), R = 200 µm (blue) and R = 250 µm (green).

Taking into account the minimum FSR value limited by the experimental setup and the waveguide propagation loss of 3 dB/cm ± 0.5 dB/cm, racetrack resonators with 5 different bending radius (R = 50 to 250 µm with a step of 50 µm) have been fabricated. Figure 2(c) shows the transmittance spectra of fabricated racetrack resonators. Clear resonances have been observed over 900 nm at a wavelength range of 8 µm, with an extinction ratio of 10 dB around the critical coupling condition. The minimum -3 dB bandwidth is measured as 2.5 nm at 8.05 µm leading to a maximum loaded quality factor of 3200.

It is worth to note that the linewidth of the used QCL is specified to be below 1 cm^{-1} (i.e. below 6.5 nm at 8 µm wavelength). Furthermore, the measurement has been performed with a step of 1 nm which is the maximum resolution of the laser. This fact can limit the maximum value of the measured Q-factor. It is thus interesting to evaluate the intrinsic quality factor of the resonators which is limited only by the waveguide loss and given by the following equation:

$$Q_{\text{int}} = \frac{2\pi \times n_g \times 4.34}{\lambda_{[\mu m]} \times 100 \times \alpha_{[dB/cm]}} \tag{2}$$

where n_g is the group index. Taking into account the waveguide propagation losses of 3 dB/cm, the calculated intrinsic Q-factor is at a magnitude of 10^4.

4. CONCLUSIONS

In conclusion, we demonstrated Bragg-grating-based Fabry-Perot cavities and racetrack resonators operating in the long-wave MIR region at a wavelength range of 8 µm. The resonance of FP cavity is demonstrated up to 8.4 µm with a maximum loaded Q-factor of 2200 measured at 7.95 µm. Moreover, in terms of racetrack resonators, a bandwidth of over 900 nm resonances have been measured with a loaded Q-factor of 3200 at

8.05 µm. This first demonstration of resonant structure at such large wavelength in the MIR wavelength range open the path towards the further implementation of advanced LWIR photonics integrated circuits.

ACKNOWLEDGEMENTS

European Research Council (ERC) under the European Union's Horizon 2020 research and innovation program (N°639107-INsPIRE). Partial support is provided also by the TEINVEIN project funded by POR FESR 2014-2020 (ID: 242092) and by the European Union Horizon 2020 FET project microSPIRE (ID: 766955). The fabrication of the device was performed at the Plateforme de Micro-Nano-Technologie/C2N, which is partially funded by the "Conseil Général de l'Essonne". This work was partly supported by the French RENATECH network.

REFERENCES

[1] H. Lin, Z. Luo, T. Gu, L. C. Kimerling, K. Wada, and A. Agarwal, "Review article Mid-infrared integrated photonics on silicon : a perspective," **7**(2), 393–420 (2018).

[2] J. Depciuch, E. Kaznowska, I. Zawlik, R. Wojnarowska, M. Cholewa, P. Heraud, and J. Cebulski, "Application of Raman Spectroscopy and Infrared Spectroscopy in the Identification of Breast Cancer," Appl. Spectrosc. **70**(2), 251–263 (2016).

[3] Y. Zou, S. Chakravarty, C.-J. Chung, X. Xu, and R. T. Chen, "Mid-infrared silicon photonic waveguides and devices [Invited]," Photonics Res. **6**(4), 254 (2018).

[4] J. M. Ramirez, Q. Liu, V. Vakarin, J. Frigerio, A. Ballabio, X. Le Roux, D. Bouville, L. Vivien, G. Isella, and D. Marris-Morini, "Graded SiGe waveguides with broadband low-loss propagation in the mid infrared," Opt. Express **26**(2), 870 (2018).

[5] Q. Liu, J. M. Ramirez, V. Vakarin, X. Le Roux, C. Alonso-Ramos, J. Frigerio, A. Ballabio, E. Talamas Simola, D. Bouville, L. Vivien, G. Isella, and D. Marris-Morini, "Integrated broadband dual-polarization Ge-rich SiGe mid-infrared Fourier-transform spectrometer," Opt. Lett. **43**(20), 5021 (2018).

[6] D. Marris-Morini, V. Vakarin, J. Manel Ramirez, Q. Liu, A. Ballabio, J. Frigerio, M. Montesinos, C. Alonso-Ramos, X. Le Roux, S. Serna, D. Benedikovic, D. Chrastina, L. Vivien, and G. Isella, "Germanium-based integrated photonics from near-to mid-infrared applications," Nanophotonics **7**(11), 1781–1793 (2018).

[7] Q. Liu, J. M. Ramirez, V. Vakarin, X. Le Roux, J. Frigerio, A. Ballabio, E. Talamas Simola, C. Alonso-Ramos, D. Benedikovic, D. Bouville, L. Vivien, G. Isella, and D. Marris-Morini, " On-chip Bragg grating waveguides and Fabry-Perot resonators for long-wave infrared operation up to 8.4 µm," Opt. Express. Accepted.

[8] J. M. Ramirez, Q. Liu, V. Vakarin, X. Le Roux, J. Frigerio, A. Ballabio, C. Alonso-Ramos, E. Talamas Simola, L. Vivien, G. Isella, and D. Marris-Morini, "Broadband integrated racetrack ring resonators for long-wave infrared photonics," Submitted Opt. Lett.